

Two-dimensional Two-frequency NQR Spectroscopy *

V. S. Grechishkin and N. Ja. Sinjavsky

Department of Physics, Kaliningrad State University, Kaliningrad, Russia

Z. Naturforsch. **47 a**, 430–438 (1992); received July 18, 1991

Two-dimensional NQR spectroscopy is experimentally accomplished by direct detection; forbidden transitions are also recorded. Two-dimensional spectra with cross-peaks are used in assigning lines in complex spectra.

A method is described of increasing the ^{14}N NQR sensitivity by saturating the line ν_0 whilst observing the NQR at a frequency ν_- . The presence of a low magnetic field is shown to improve the conditions for localised NQR observations.

Introduction

Advances in NQR spectroscopy are due to the development of pulse methods: The two-frequency method [1] takes first place and allows us to get additional information about non-linear spin-system.

It is pointed out in this paper that two-frequency methods based on NQR are equivalent to the two-dimensional frequency NMR experiment [2]. The non-diagonal signals of a two-dimensional spectrum, pointing to the presence of magnetization transfer between different states, are equivalent to the additional signals of the two-frequency quadrupolar echo.

Two-dimensional (2D) spectroscopy in high resolution NMR in high magnetic fields is well developed [3]. This is two-dimensional correlation spectroscopy (COSY), where two spectra correlate with each other on the basis of connections, or in other cases where exchange or cross-relaxation transitions cause cross-peaks in the 2D-NMR spectrum.

2D-spectroscopic methods have been successfully applied to NQR and NMR in zero-field [4, 5], though field cycling techniques and indirect detection complicate the apparatus and extend the time of the experiment.

The objectives of this article are to establish the relations between the appearance of two-frequency signals in the “square” programme and cross-peak coordinates in 2D spectra, the experimental conditions for two-dimensional NQR spectroscopy by di-

rect detection and the investigation of the possibility of improving the conditions of localized NQR observation by the presence of a low magnetic field.

1. Two-frequency Method

In the case of spins $I = 1, 5/2, 7/2$, or $9/2$, when there is a nonequidistant set of energy levels, simultaneous excitation of two neighbouring transitions gives rise to additional spin echo signals. Recently the two-frequency method has been successfully applied to the unambiguous assignment of lines in complex multiplet NQR spectra [1, 6, 7]. For nitrogen nuclei ($I = 1$), the weak signals require signal accumulation [8], so the choice of the best conditions to conduct the experiment using the two-frequency method is of paramount importance.

We are going to present the results of calculations of the spin-echo signals for the main two-frequency programme. The calculations have been done by the density matrix method [9] in the first order approximation. The radiofrequency coils of the two transmitters are considered to be parallel in [7], for example one and the same coil is used. Their axes are oriented arbitrarily with respect to the direction of the principal axes of the electric field gradient tensor. θ and φ are the polar angles in that frame of the direction of the radiofrequency field B_1 . The values of $\langle I_q \rangle$, where $q = x, y, z$, are now calculated.

Let us consider the case $I = 1$, in which the sample is subjected to two radiofrequencies ω_+ and ω_- . We write the radiofrequency field as follows

$$B = 2B_1 [\cos(\omega_+ t + \xi_1) + \cos(\omega_- t + \varphi_1)] . \quad (1)$$

* Presented at the XIth International Symposium on Nuclear Quadrupole Resonance Spectroscopy, London, U.K., July 15–19, 1991.

Reprint requests to Prof. V. S. Grechishkin, Department of Physics, Kaliningrad State University, Kaliningrad, Russia.

0932-0784 / 92 / 0100-0430 \$ 01.30/0. – Please order a reprint rather than making your own copy.



Dieses Werk wurde im Jahr 2013 vom Verlag Zeitschrift für Naturforschung in Zusammenarbeit mit der Max-Planck-Gesellschaft zur Förderung der Wissenschaften e.V. digitalisiert und unter folgender Lizenz veröffentlicht: Creative Commons Namensnennung-Keine Bearbeitung 3.0 Deutschland Lizenz.

Zum 01.01.2015 ist eine Anpassung der Lizenzbedingungen (Entfall der Creative Commons Lizenzbedingung „Keine Bearbeitung“) beabsichtigt, um eine Nachnutzung auch im Rahmen zukünftiger wissenschaftlicher Nutzungsformen zu ermöglichen.

This work has been digitalized and published in 2013 by Verlag Zeitschrift für Naturforschung in cooperation with the Max Planck Society for the Advancement of Science under a Creative Commons Attribution-NoDerivs 3.0 Germany License.

On 01.01.2015 it is planned to change the License Conditions (the removal of the Creative Commons License condition “no derivative works”). This is to allow reuse in the area of future scientific usage.

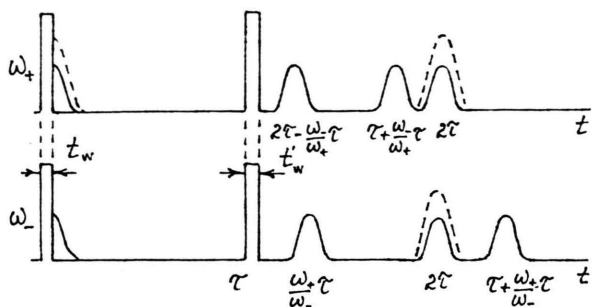


Fig. 1. The two-frequency "square" program for spin $I=1$.

Here ξ_1 and φ_1 are the initial phases of the first radio-frequency pulses. The initial phases of the second radiofrequency pulses are ξ_2 and φ_2 . Then, for the case of the so-called "square" programme (Fig. 1), we obtain the following expressions for two-frequency echo signals at frequencies ω_+ , ω_- and ω_0 :

$$\langle I_q \rangle = \sum_i \left[S_{\omega_j} \left(\frac{\omega_j + \omega_i}{\omega_j} \tau \right) + S_{\omega_j} \left(\frac{\omega_j - \omega_i}{\omega_j} \tau \right) \right] + S_{\omega_j}(\tau), \quad (2)$$

where i and j take the values $+$, $-$, and 0 ; $q=x$ for $j=+$, $q=y$ for $j=-$, and $q=z$ for $j=0$. Here $S_{\omega_j} \left(\frac{\omega_j + \omega_i}{\omega_j} \tau \right)$ refers to the time $\frac{\omega_j + \omega_i}{\omega_j} \tau$.

Echo signals appearing at times smaller than τ do not have physical meaning as they appear before the reasons which cause them, i.e. before the application of the second radiofrequency pulse, and must be omitted in (2). The signal induced in the coil of the spectrometer will be equal to

$$S(\tau, t) = \langle I_x \rangle \sin \theta \cos \varphi + \langle I_y \rangle \sin \theta \sin \varphi + \langle I_z \rangle \cos \theta. \quad (3)$$

In order not to write cumbersome expressions, we do not calculate the averaged responses for a powder; we confine ourselves to the case $\theta = \varphi = \pi/4$ and take for simplicity that the angles of rotation of the sample magnetization after the radiofrequency pulses are $\alpha_1 = \alpha_2 = \pi/2$. Then the signal registered by the two-frequency spectrometer at the excitation frequencies (ω_+ and ω_-) after the second radiofrequency pulse will be equal to

$$S(\tau, t) = \frac{\hbar N}{12 \sqrt{2} kT} \left\{ (\omega_+ - \omega_-) \sin [\omega_+(t - 2\tau)] + (\omega_+ + \omega_-) \sin \left[\omega_+ \left(t - 2\tau + \frac{\omega_-}{\omega_+} \tau \right) \right] \right.$$

$$\begin{aligned} &+ (-\omega_+ + \omega_-) \sin \left[\omega_+ \left(t - \tau - \frac{\omega_-}{\omega_+} \tau \right) \right] \\ &+ (-\omega_+ + \omega_-) \sin [\omega_-(t - 2\tau)] \\ &+ (\omega_+ + \omega_-) \sin \left[\omega_- \left(t - \frac{\omega_+}{\omega_-} \tau \right) \right] \\ &\left. + (\omega_+ - \omega_-) \sin \left[\omega_- \left(t - \tau - \frac{\omega_+}{\omega_-} \tau \right) \right] \right\}. \quad (4) \end{aligned}$$

The solution of the problem for $I=5/2$ according to the "square" programme (Fig. 2) by the matrix density method in the one-frequency approximation gives rise to signals at frequencies ω_1 and ω_2 (1):

$$\begin{aligned} S(\tau, t) = A \{ &(\sin \alpha \cos \alpha + 12 \sin \alpha) \\ &\cdot [0.164 \sin^2 \alpha' \sin \omega_2(t - 2\tau) + 0.261 (\cos \alpha' - 1) \\ &\cdot \cos \alpha' \sin \omega_1(t - 3\tau)] + (\sin 2\alpha - 15 \sin \alpha) \\ &\cdot [-0.21 \sin^2 \alpha' \sin \omega_1(t - 2\tau) \\ &\quad - 0.128 (\cos \alpha' \sin \omega_2(t - \frac{3}{2}\tau))] \\ &+ [2.66 \cos \alpha (\cos \alpha - 1) \\ &\quad + 4.1 (\cos \alpha - 1) + 0.585 \sin^2 \alpha] \\ &\cdot (\cos \alpha' - 1) \sin \alpha' [\sin \omega_1(t - 4\tau) \\ &\quad - 0.63 \sin \omega_2(t - \frac{5}{2}\tau)] \}, \quad (5) \end{aligned}$$

where

$$\alpha = \frac{\sqrt{13}}{2} \gamma B_1 t_w, \quad \alpha' = \frac{\sqrt{13}}{2} \gamma B_1 t'_w.$$

Expressions (4) and (5) give only the intensities and times of appearance of the additional echo signals, and they say nothing about the form of the signals and the relaxation times.

The experimental detection of two-frequency NQR signals by direct methods is accomplished by existing techniques, although the analysis of these signals in the time domain can not be successfully performed. NQR Fourier-spectroscopy has a higher sensitivity and resolution so that it is natural to apply Fourier methods to two-frequency signal analysis.

2. Two-dimensional NQR Spectra

In general 2D NQR spectroscopy uses the same two-dimensional experiments as in high resolution NMR. The first experimental two-dimensional NMR

and NQR spectra in zero-field for deuterium have been published in (4), and for the case of field excitation by low frequency pulses in (5).

Two-dimensional NMR and NQR ($I = 1$) spectroscopy in zero field turns out to be very convenient for complex spectra analysis. Despite the fact that the

technique combined with field cycling [10] is attractive for ^{14}N and ^2H spectroscopy in the frequency range below 1 MHz, two-dimensional spectroscopy in zero field requires very much time, since only one point of the two-dimensional function $S(t_1, t_2)$ is registered in one cycle, which besides may require storage.

To clarify the possibility of using all ^{14}N signals to correlate the lines in a complex cross-peak spectrum, we have modelled a two-dimensional spectrum obtained by excitation of the spin system by magnetic field video-pulses. It is assumed that the timing diagram of the two-dimensional NQR (Fig. 2a) experiment for $I = 1$ in zero-field corresponds to the case discussed in [2]. It was supposed in the calculation that the two-dimensional signal interferogram of the nitrogen nuclei $S(t_1, t_2)$ is not distorted by indirect detection, and that dipole-dipole interactions in zero-field are absent. The intensities $S(t_1, t_2)$ were calculated by means of the formula

$$S(t_1, t_2) = Sp[\varrho(0) \exp(-i\zeta H_1) \exp(-iH_Q t_2) \cdot \exp(-i\zeta' H_1) \exp(-iH_Q t_1) \exp(-iH_1 \zeta) \cdot \varrho(0) \exp(iH_1 \zeta) \exp(iH_Q t_1) \exp(i\zeta' H_1) \cdot \exp(iH_Q t_2) \exp(i\zeta H_1)], \quad (6)$$

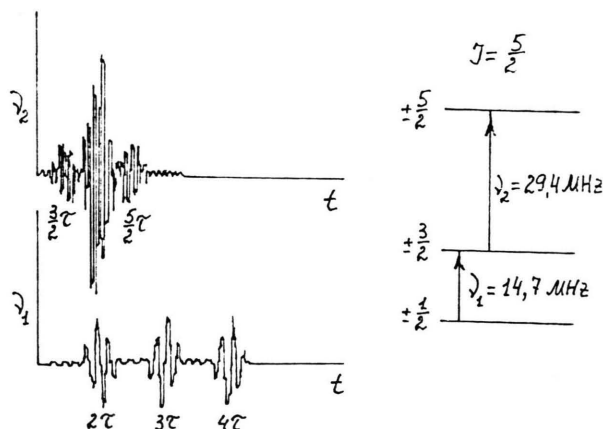


Fig. 2. The two-frequency spin echo signals for ^{127}I nuclei in CdI_2 , with $t_w = 10$ ms, $t_w' = 20$ ms, $T_2^* = 50$ ms. For ν_1 , $T_2 = 350$ ms for the main and $T_2 = 300$ ms for the additional echo signals; for ν_2 , $T_2 = 1600$ ms for the main and $T_2 = 300$ ms for the additional echo signals.

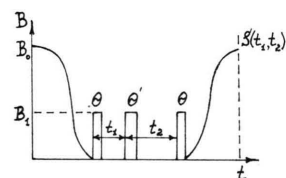
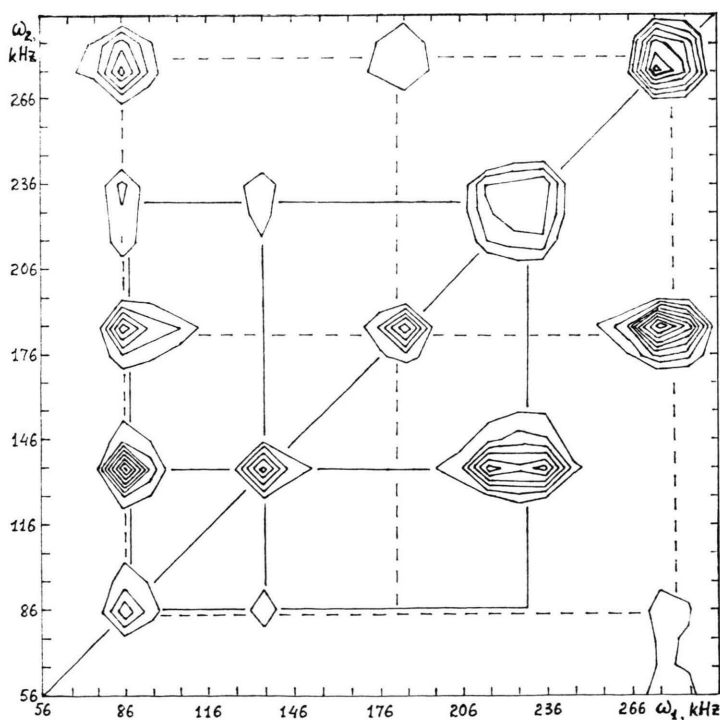


Fig. 2a. The timing diagram of the 2D NQR experiment in zero-field.

Fig. 3. Topogram of a calculated two-dimensional NQR spectrum.



where H_Q is the quadrupolar Hamiltonian interaction, H_1 is the Hamiltonian expressing the interaction with the constant field B_1 , ξ and ξ' are the pulse lengths of the magnetic field which initiate and interrupt the evolution of the spin system evolution, and $\varrho(0)$ is the equilibrium density matrix in zero field.

In Fig. 3 a two-dimensional spectrum is shown, calculated for the case in which there are two nonequivalent positions of the nuclei in the sample. The lines on the diagonal correspond to the one-dimensional spectrum. Cross-peaks related to the different equivalent positions are connected by the dotted and continuous lines, respectively. As it is seen in the figure, one row of cross peaks is absent because of their low intensities at certain values of ξ and ξ' . Here $eQq_{zz}^{(1)} = 300$ kHz, $\eta^{(1)} = 0.6$. This absence may make it impossible to locate lines by means of the cross-peaks for ν_+ and ν_- , as was suggested in [4, 5], and we suggest using the available cross-peaks for ν_0 for this purpose, as shown in Figure 3.

To construct the two-dimensional spectrum, a special program has been used. The two-dimensional function $S(t_1, t_2)$ is calculated at 64×64 points, without powder averaging, on a "Compan" PC in about 25 minutes. The two-dimensional complex Fourier transformation of the function represented by 128×128 points lasted about 4 minutes, and the preparation of the 50×50 two-dimensional graph of the function $S(\omega_1, \omega_2)$ took about 30 minutes.

In direct pulse detection methods the two-dimensional function response $S(\tau, t)$ after two radiofrequency pulses is registered, and Fourier transformation then gives the two-dimensional spectrum $S(\omega_1, \omega_2)$. Here τ is the delay between pulses and t is the time of application of the current following the second pulse. Figure 4 illustrates the experimental two-dimensional ^{14}N spectrum recorded by such a mode at 77 K for $\text{CO}(\text{NH}_2)_2$ at the frequency $\nu_+ = 2917.7$ kHz. The function $S(\tau, t)$ was recorded in the experiment at 128×128 points to derive this spectrum. The two-dimensional spectral line asymmetry is well seen and is due to the difference in relaxation times T_2^* and T_2 . The corresponding one-dimensional spectrum of this sample is represented in Figure 5.

The block-diagram of the apparatus used for recording two-dimensional two-frequency NQR spectra by direct methods is represented in Figure 6. The pulse-coherent NQR spectrometer has two independent channels for excitation and recording of the two-frequency spin echo signals. The working frequencies

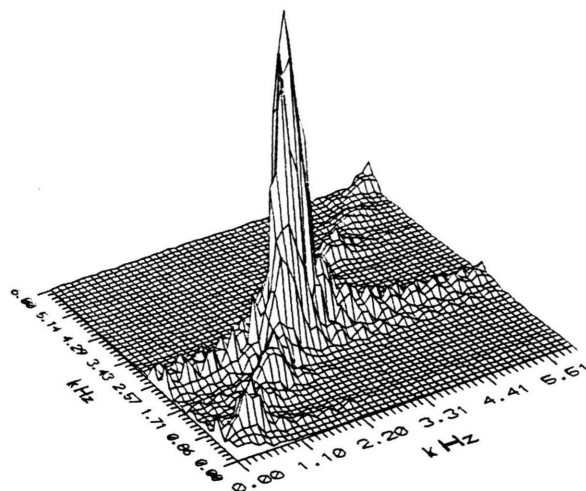


Fig. 4. Two-dimensional ^{14}N NQR spectrum from urea.

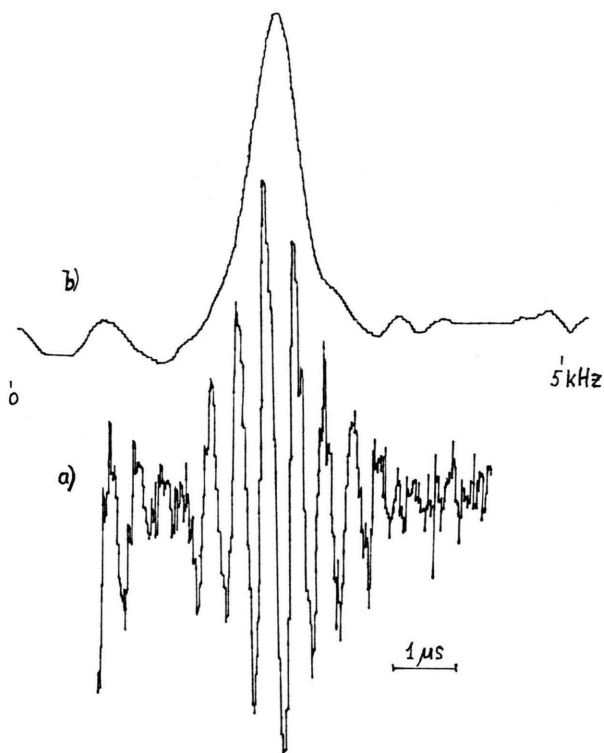


Fig. 5. Echo signal from urea at a frequency $\nu_+ = 2911$ kHz at 77 K, with $t_w = 50$ ms, $t'_w = 100$ ms, $\Delta t = 20$ ms (a) and FT from half echo (b) using 4096 signal points.

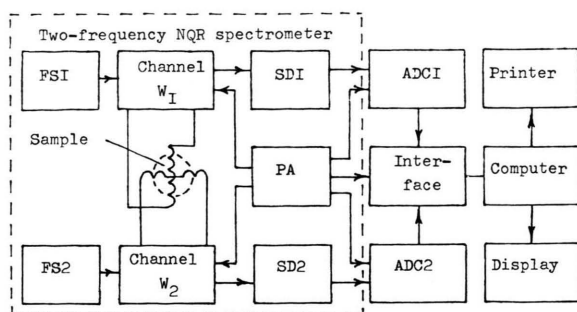


Fig. 6. Block-diagram of a two-dimensional two-frequency NQR spectrometer.

are supplied by Frequency Synthesizers 1 and 2 (frequency synthesizers 46–31). The programming apparatus produces all the pulses and controls the functioning of the whole spectrometer. The signals at frequencies ω_1 and ω_2 of neighbouring transitions are detected by the synchronous detectors SD1 and SD2 and digitized by the converters ADC1 and ADC2. The two-frequency spin echo signals of both transitions representing the time response of the sample to the two-frequency excitation by the “square” program, for example, are fed to the main memory of on “Iskra-1030” micro-SPC via an interface.

One line of the two-dimensional function $S(\tau, t)$ corresponding to a given τ is fixed during one period of measurement. The program (PA) changes τ between pulses by the necessary step, allowing us to register the whole matrix $S(\tau, t)$.

The two-dimensional spectrum recorded in an analogous manner from the NQR response to two-frequency excitation by the “square” program [10] will be completely equivalent to the cross-peak spectrum which has been discussed above. Vice versa, if we know the position and cross-peak intensities in the two-dimensional spectrum, we can determine the time of appearance and two-frequency signal intensities in the “square” program.

It is known that the two-frequency method [1] can be used to increase the signal/noise ratio in nuclear quadrupole resonance [2]. However, in localized NQR, when the sample is adjacent to a flat radiofrequency coil, two-frequency methods have been used before. As an example of this kind of investigation we take crystals of $N_3(CH_2)_3(NO_2)_3$. In this sample at 300 K the strongest ^{14}N NQR lines can be observed at frequencies of $\nu_+ = 5192$ kHz; $\nu_- = 3410$ kHz and $\nu_0 = 1782$ kHz [11]. If the transition at a frequency ν_0

[12] is saturated by means of a radiofrequency pulse, then it follows that

$$\frac{n_-^s}{n_-^\infty} = \frac{3}{3 - \eta}, \quad (7)$$

where n_-^s is the transition intensity at frequency ν_- with saturation at frequency ν_0 , n_-^∞ is the transition intensity at frequency ν_- without saturation and η is the asymmetry parameter. For $N_3(CH_2)_3(NO_2)_3$, $\eta = 0.63$ so that $n_-^s/n_-^\infty = 1.265$.

The change in signal intensity in two-frequency methods is mainly determined by the relaxation time of the sample and by the manner of the two-frequency signal excitation. The influence of the latter lies in the mixing of the relaxation characters of the excited NQR transitions [2].

Two-frequency saturation experiments are conducted on an NQR pulse spectrometer with a pair of flat surface coils [2]. The length of the saturating radiofrequency pulse at frequency ν_0 was chosen to be 1 ms and the pulse amplitude 10 G. The pulses at frequency ν_- had a length of 30 ms, with a distortion of 0.25 kHz caused the induction signal appearance. 10^4 induction signals were stored in the periods between the ν_- pulses in a total time of 1 s by means of the “Compan” PC, which increased the signal/noise ratio by a factor of hundred. The introduction of a preliminary saturating pulse at frequency ν_0 also increased the signal/noise ratio. Observation at the NQR frequency ν_+ (for which $T_2 = 1.3$ ms, $T_1 \sim 1.3$ ms at 300 K) gave the possibility of checking all the theoretical correlations in this two-frequency experiment.

Some improvements in localized NQR have been obtained by the presence of a low magnetic field across the sample generated by a U-shaped solenoid, since the time T_2 is increased. Fast Fourier transformation of the induction signals has been performed in an external magnetic field; Figure 7 shows ^{14}N NQR signals in $N_3(CH_2)_3(NO_2)_3$ and $N_4(CH_2)_6$ at 300 K in a magnetic field perpendicular to the radiofrequency coil axis.

The sensitivity to the external magnetic field depends mainly on η . The width of the ν_0 lines in $C_3H_6N_6O_6$ is increased in a field of 70 G by a factor of two compared to their width in zero field (~ 0.3 kHz). In hexamethylenetetramine, when the sample is not subject to the magnetic field, two signals of different intensities are seen in the NQR spectrum. The splitting of the ^{14}N NQR line is determined here by the local field

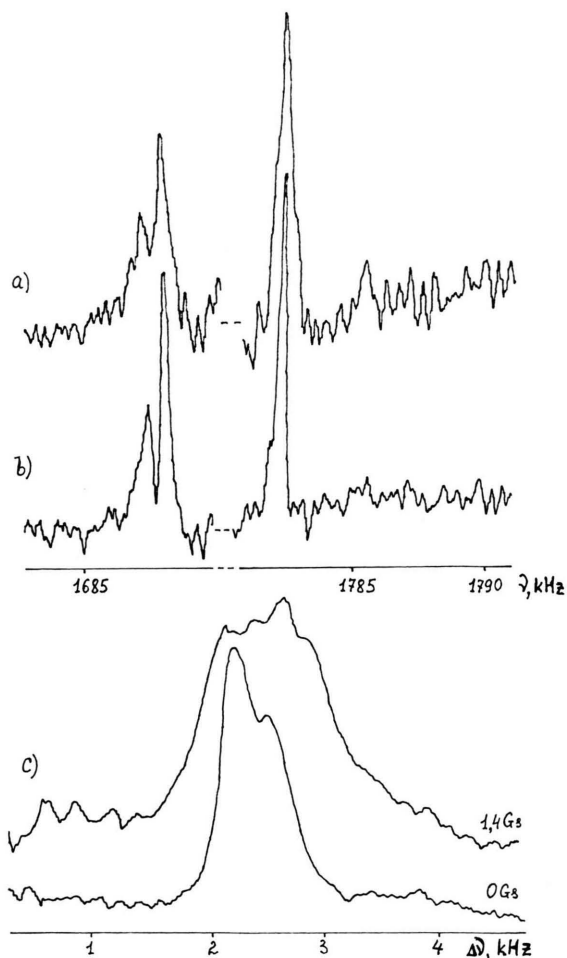


Fig. 7. Lines $\nu_0^{(1)} = 1688$ kHz, $\nu_0^{(2)} = 1689$ kHz and $\nu_0^{(3)} = 1782$ kHz in $C_3H_6N_6O_6$: a) $B = 70$ G; b) $B = 0$; c) the influence of a constant magnetic field on the ^{14}N NQR lines in $C_6H_{12}N_{14}$.

generated by the CH_2 protons in this molecule. A broadening of the spectrum combined with a small displacement towards higher frequency take places as the magnetic field is increased, as is seen in Figure 7. Practically this does not contradict the results of the theoretical analysis made in paper [13], where it is stated that in the presence of an external magnetic field the line is broadened, is decreased in amplitude and is displaced in frequency. The amplitude and the maximum frequency displacement are most easily determined from experiment. It is however difficult to measure the change in frequency with magnetic field as the broadened line is asymmetric. In low magnetic fields the ν_+ line increases in frequency as a quadratic

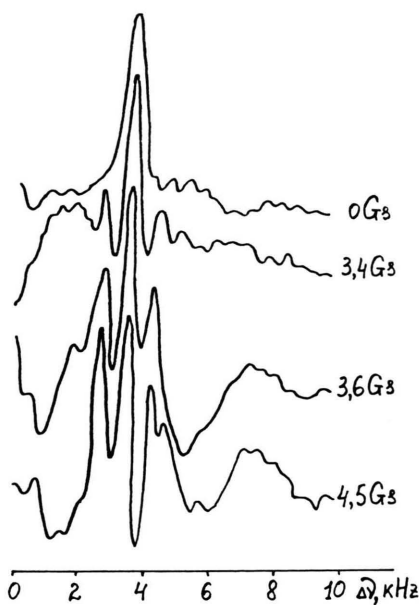


Fig. 8. Influence of a constant magnetic field of 210 Hz on the ^{14}N NQR spectrum of hexamethylenetetramine.

function of the field [13]. The line ν_- may have either positive or negative frequency displacements, depending on the asymmetry parameter η and the angle α between the radiofrequency and constant magnetic field. A line with $\eta < 0.7$ has a negative displacement for $\alpha = 90^\circ$ and low magnetic field, but in higher fields most ν_- lines show a positive displacement before disappearance because of broadening.

The Zeeman effect in ^{14}N NQR has been investigated by means of an alternating magnetic field applied to the sample perpendicular to the radiofrequency field. The spectrometer radiofrequency pulses were synchronized with the magnetic field oscillations of the modulating coil. Figure 8 illustrates the changes in the ^{14}N NQR spectrum of hexamethylenetetramine when the sample is placed in an alternating magnetic field with a frequency of 210 Hz with different magnetic field amplitudes. In this case, we expect the spectrum to contain the main line displaced by a frequency $\Delta\nu = 3.6$ kHz due to the distortion of the spectrometer frequency together with sidebands of frequencies $\Delta\nu \pm n\Omega/2\pi$, where $\Omega/2\pi$ is the modulating magnetic field frequency and n is an integer. For the case illustrated in Fig. 8, $\Omega/2\pi = 2 \cdot 210$ Hz, since the induction signal amplitude changed twice during the period of modulating voltage. In reality it is possible to observe only lines at $\Delta\nu \pm 3\Omega/2\pi$ ($\Delta\nu = 3.6$ kHz). However, in-

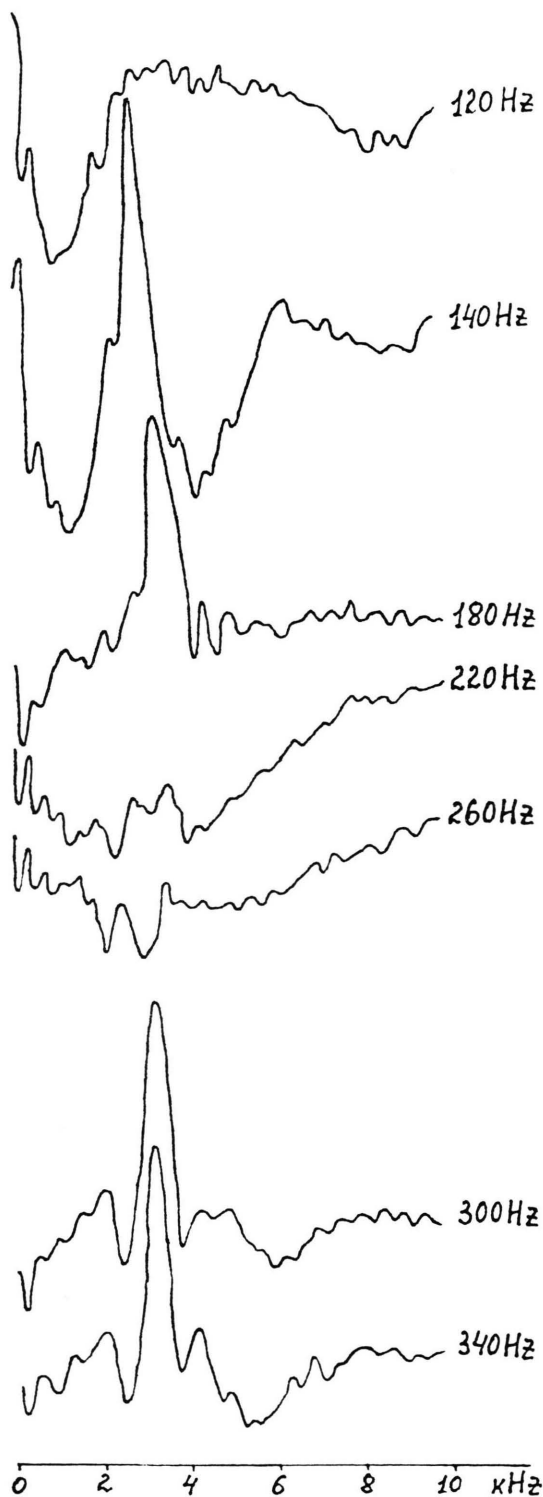


Fig. 9. Changes in the ^{14}N NQR spectrum of hexamethylenetetramine with change of the modulating magnetic field frequency.

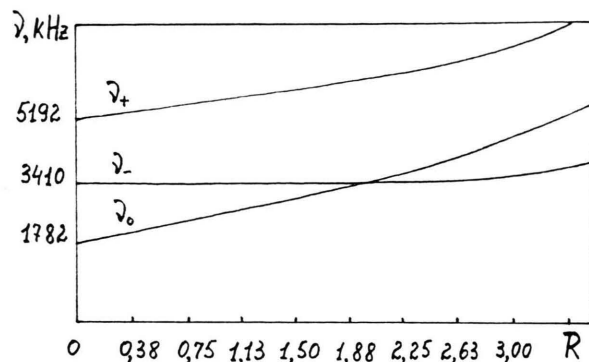


Fig. 10. Dependence of the quadrupole energy levels for spin $I=1$ on the magnetic field.

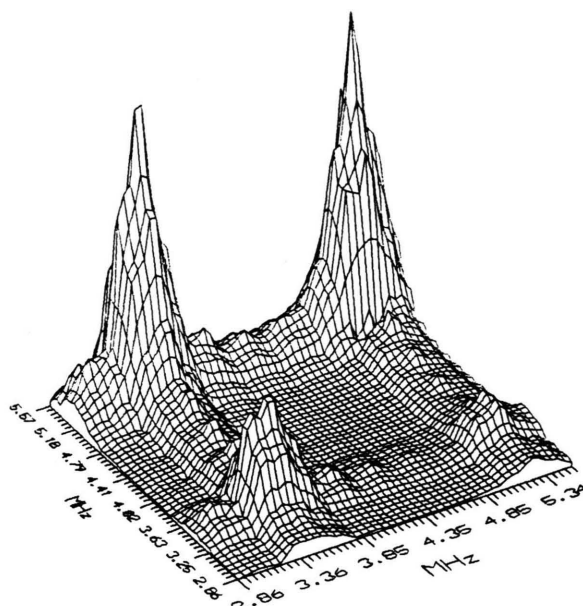
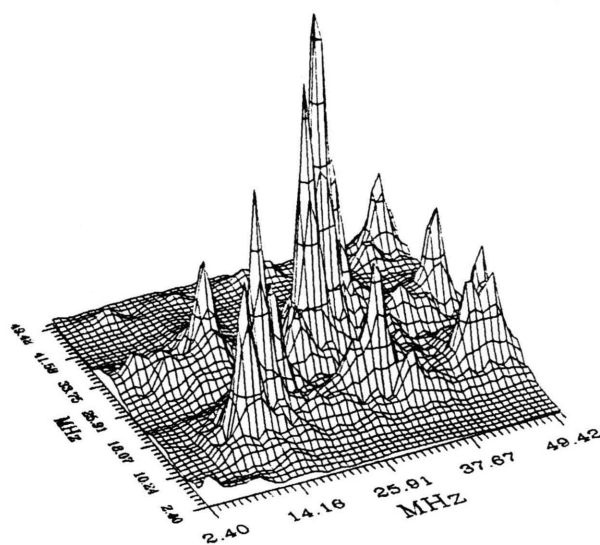
crease of the modulating field amplitude increases the amplitude of the sidebands. At low modulation frequencies (0 to 120 Hz) the signal is completely suppressed because of line broadening (Figure 9). With frequency increase the resistance of the modulating coil increases, the field amplitude decreases (at constant supply voltage) and the amplitudes of the main NQR line and its sidebands increase. Above 200 Hz, the suppression of the NQR signals may be explained by the closeness of the modulation frequency to the value of the ^{14}N splitting in hexamethylenetetramine (~ 250 Hz).

Figure 10 shows the theoretical dependence of the frequencies ν_+ , ν_- and ν_0 in powdered $\text{N}_3(\text{CH}_2)_3(\text{NO}_2)_3$ on an external magnetic field; $R = \frac{4\mu B_0}{eQq_{zz}}$, where μ is the magnetic moment of the ^{14}N nucleus, B_0 is the external field, eQq_{zz} is the quadrupole coupling constant, and the dependence has been calculated on a "Compan" PC at 25 000 angular positions. The experiment has confirmed that the line ν_- does not depend on R but that the lines ν_0 and ν_+ depend on the magnetic field.

We return to a consideration of the two-frequency spin echo for ^{14}N nuclei [10]. The times of appearance of two-frequency echo signals for ^{14}N nuclei on the "square" program [1, 10] are shown in Table 1. Fourier transformation of the function $S(\tau, t)$, where τ is the time interval between pulses, gives the two-dimensional NQR spectrum. From the table it is seen that the two-dimensional spectrum cross-peaks are equivalent to the times of signal appearance in the two-frequency method. Figure 11 shows the two-dimensional ^{14}N NQR spectrum of $\text{C}_3\text{H}_6\text{N}_6\text{O}_6$. The diagonal section corresponds to the one-dimensional

Table 1.

The excitation frequency	Detection frequency	The times of appearance of two-frequency echo signals	The coordinates of peaks of the two-dimensional spectrum
v_+, v_-	v_+	0	$v_+, 0$
		τ	v_+, v_+
		2τ	$v_+, 2v_+$
		$2\tau - \frac{v_-}{v_+} \tau$	$v_+, v_+ + v_0$
		$\tau + \frac{v_-}{v_+} \tau$	$v_+, v_+ + v_-$
v_+, v_0	v_-	0	$v_-, 0$
		τ	v_-, v_-
		2τ	$v_-, 2v_-$
		$\tau + \frac{v_+}{v_-} \tau$	$v_-, v_- + v_+$
		$\frac{v_+}{v_-} \tau$	v_-, v_+
v_-, v_0	v_0	0	$v_0, 0$
		τ	v_0, v_0
		$\frac{v_+}{v_0} \tau$	v_0, v_+
		2τ	$v_0, 2v_0$
		$\tau + \frac{v_+}{v_0} \tau$	$v_0, v_0 + v_+$
v_-, v_0	v_-	0	$v_-, 0$
		τ	v_-, v_-
		$\frac{v_+}{v_-} \tau$	v_-, v_+
		2τ	$v_-, 2v_-$
		$\tau + \frac{v_+}{v_-} \tau$	$v_-, v_- + v_+$
v_0, v_+	v_0	0	$v_0, 0$
		τ	v_0, v_0
		2τ	$v_0, 2v_0$
		$\frac{v_+}{v_0} \tau$	v_0, v_+
		$\tau + \frac{v_+}{v_0} \tau$	$v_0, v_0 + v_+$

Fig. 11. Two-dimensional ^{14}N NQR spectrum of $\text{C}_3\text{H}_6\text{N}_6\text{O}_6$.Fig. 12. Two-dimensional ^{127}J NQR spectrum of CdI_2 .

spectrum (lines v_+ and v_-). The triplet structure of the lines due to the three nonequivalent nitrogen positions is not shown because of the large scale. The cross peaks intensities depend on the length of the excitation pulses. With better resolution, the two-dimensional NQR spectrum of $\text{N}_3(\text{CH}_2)_3(\text{NO}_2)_3$ gives rise to cross-peaks, enabling unambiguous line correla-

tions to the definite nonequivalent positions in the crystal to be made, which is equivalent to a two-frequency experiment. Thus the application of two-frequency methods in localized NQR shows new possibilities for increasing the signal/noise ratio, and the transition to two-dimensional spectra suggests new ways of correlating NQR lines to definite nonequivalent positions of nitrogen nuclei in the crystal.

Finally, we consider the case of spin quantum number $I = 5/2$ with $\eta = 0$, where the transition $\pm 1/2 \rightarrow \pm 5/2$ has zero transition probability and is impossible to detect [1]. We have excited the transitions $\pm 1/2 \rightarrow \pm 3/2$ (at 14.7 MHz) and $\pm 3/2 \rightarrow \pm 5/2$ (at 29.4 MHz) for ^{127}I in CdI_2 by means of two pulse pairs, with the lengths t_w and t'_w , separated by a time interval ("square" program [2]). The spin-system response at frequencies ω_1 and ω_2 after the second pulses $S_1(\tau, t)$ and $S_2(\tau, t)$ were entered into a "Compan" PC, summed, and the two-dimensional complex Fourier transformation was done from this function. Here t is the time counted from the beginning of the

second pulse. The two-dimensional spectrum $S(\omega_1, \omega_2)$ was constructed and printed by means of the program "Surfer". Figure 12 represents the ^{127}I spectrum in CdI_2 ; at the same time as transitions at frequencies ω_1 (14.7 MHz) and ω_2 (29.4 MHz) in the main diagonal, a transition at a frequency ω_3 (44.1 MHz) is seen, which in the one-frequency version is absent. In addition cross-peaks with coordinates (14.7; 29.4) MHz, (29.4; 14.7) MHz are seen, including those corresponding to the forbidden transitions (14.7; 44.1) MHz and (29.4; 44.1) MHz. The appearance of the forbidden transitions in a two-dimensional spectrum is caused by mixing of quantum states by two-frequency excitation. Both the main signals and the two-dimensional spectrum cross-peaks have intensities and phases determined by the length and the initial phases of the excitation pulses. The excitation of forbidden transitions and the presence of cross-peaks in cases where there are several nonequivalent positions in the sample allows us to identify the NQR lines unambiguously.

- [1] V. S. Grechishkin, Nuclear Quadrupole Interactions in Solids, Nauka, Moscow 1973.
- [2] V. P. Anferov, V. S. Grechishkin, and N. Ja. Sinjavsky, Nuclear Spin Resonance, Modern Methods, State University, Leningrad 1990.
- [3] R. R. Ernst, D. Bodenhausen, and A. Wokaun, Principles of Nuclear Magnetic Resonance in One- and Two-dimensions, Mir, Moscow 1990.
- [4] A. M. Thayer, J. M. Millar, and A. Pines, Chem. Phys. Letters **129**, 55 (1986).
- [5] R. Kreis, Nullfeld NMR und NQR Spektroskopie mit gepulster Anregung, Dissertation, Technische Hochschule, Zürich 1989.
- [6] V. S. Grechishkin and E. M. Shishkin, Two-frequency Effects in NQR. Proc. of Higher Education. Physica **3**, 82 (1973).
- [7] E. O. Azizov, V. S. Grechishkin, and U. M. Lugansky, J. Phys. Chem. **53**, 58 (1979).
- [8] I. A. Safin and D. Ja. Osokin, Radiospectroscopy, Science, Moscow 1973.
- [9] T. P. Das and E. L. Hahn, Sol. State Phys., Suppl. **1** (1958).
- [10] V. S. Grechishkin, V. P. Anferov, and N. Ja. Sinjavsky, Adv. in NQR **5**, 1 (1983).
- [11] R. J. Karpowitz and T. B. Brill, J. Chem. Phys. **87**, 2109 (1983).
- [12] V. S. Grechishkin, G. V. Mozshukhin, N. Ja. Sinjavsky, and E. V. Urepina, Two-frequency saturation in ^{14}N NQR, Proc. Higher Education, Physica 1988.
- [13] S. Pissanetzky, J. Chem. Phys. **59**, 4197 (1973).